Resilience Enhancement via Automatic Switching considering Direct Load Control Program and Energy Storage Systems

Seyed Amir Mansouri
Islamic Azad University
Tehran, Iran
amir.mansouri24@gmail.com

Emad Nematbakhsh
University of Isfahan
Isfahan, Iran
nematbakhsh.emad@hotmail.com

Mohammad Sadegh Javadi
INESC TEC
Porto, Portugal
msjavadi@gmail.com

Ahmad Rezaee Jordehi
Islamic Azad University
Rasht, Iran
ahmadrezaeejordehi@gmail.com

Miadreza Shafie-khah
University of Vaasa
Vaasa, Finland
miadreza@gmail.com

João P. S. Catalão
FEUP and INESC TEC
Porto, Portugal
catalao@fe.up.pt

2021 IEEE International Conference on Environment and Electrical Engineering and 2021 IEEE Industrial and Commercial Power Systems Europe (EEEIC / I&CPS Europe) | 978-1-6654-3613-7/21/$31.00 ©2021 IEEE | DOI: 10.1109/EEEIC/ICPSEurope51590.2021.9584609

***Abstract*—This paper presents a dynamic model to improve the resilience of the distribution network during contingent events. In this model, when an event occurs, the system operator maximizes power supply by changing the network topology as well as utilizing the direct load control (DLC) program. The model is implemented on a modified IEEE 69-bus distribution system and includes three types of residential, commercial and industrial loads. First, numerous scenarios are generated based on weather forecasting, and then the problem is solved for high-probability scenarios. It is noteworthy that industrial loads are considered as vital loads and the priority of load supply is for industrial, residential and commercial loads, respectively. The final problem is formulated as mixed-integer linear programming (MILP) problem and solved by CPLEX solver in GAMS software. The effect of dynamic topology on load supply has been investigated. In addition, the impact of using the DLC program and electrical energy storage systems (EES) systems on load supply been studied in detail.**

Keywords—Distribution feeder reconfiguration; Resilience enhancement; Direct load control Program; Renewable energy sources

I. INTRODUCTION

In recent years, the rate of natural disasters has increased due to climate change. Some of these natural disasters, such as floods and hurricanes, pose serious problems for network security. It should be mentioned that these disasters can lead to the outage of power transmission lines or generation units and subsequently cause part of the network to shut down. Therefore, supplying customers load and maintaining the system stability in these conditions has become vital. Many studies have shown that local generation units, EES systems, and proactive reconfiguration strategies lead to increased system stability under critical conditions.

In [1], a synchrophasor-based proactive reconfiguration strategy has been used to enhance the resiliency of the distribution systems against extreme weather conditions and cyber issues. The problem has been formulated as a mixed-integer linear problem (MILP) and is solved by mathematical programming techniques. The results show that in the case of industrial feeders, the proposed methodology suffers from low computational speed.

J.P.S. Catalão acknowledges the support by FEDER funds through COMPETE 2020 and by Portuguese funds through FCT, under POCI-01-0145-FEDER-029803 (02/SAICT/2017).

In [2], the schedule of sectionalizing and tie switches as well as the schedule of distributed generators are determined in a way that the resiliency of the active distribution system including the photovoltaic unit is enhanced against extreme weather conditions and natural disasters. The resiliency enhancement strategy has been developed and validated for N-1, N-2 and N-3 contingencies, so the other contingencies have been assumed impossible. In [3], the radiality constraints for distribution system reconfiguration-based resilience enhancement have been analyzed and discussed.

In [4], dynamic clustering of distribution systems and demand response (DR) have been used to enhance the resiliency of the distribution systems against extreme weather conditions. The problem has been formulated as mixed-integer nonlinear optimisation problem (MINLP) and is solved with a metaheuristic optimisation algorithm, known as the exchange market algorithm. The results indicate that the simultaneous usage of DR and distribution systems' clustering can decrease the energy not supplied (ENS) index of the system by 29.1%. In [5], DR has been used to enhance the resiliency of the active distribution systems against extreme weather conditions. The distribution system includes PV unit and the uncertainties of PV generation and demand are considered. The problem is modeled as a MILP and stochastic scenario-based method is used to deal with the uncertainties.

In [6], a unified two-stage reconfiguration strategy has been developed to enhance the resilience of the distribution systems. In the pre-event stage, the status of remotely-controlled switches and reconfiguration is done in a way that the distribution system is prepared for a possible fault caused by extreme weather conditions. In the post-event stage, system reconfiguration based on the status of remotely controlled switches is done for fast load restoration and minimizes the loss of load expectation as the resilience matric of the system. To reduce computational time and increase the computational accuracy, benders decomposition has been used in which the problem is decomposed into a master problem and several low-sized sub-problems. In [7], the reconfiguration of the distribution system and optimal location and schedule of mobile generation resources and mobile storage systems are used to enhance the resilience of the distribution system against extreme weather conditions. The proposed methodology is done in two stages; pre-event stage and post-event stage and the problem is formulated as MILP. The results indicate the significant effect of pro-active reconfiguration on the resilience of the distribution systems.

In this paper, a dynamic model for improving the resilience of the distribution network during the contingent events is presented, in which RESs and EES systems are also considered. To increase flexibility in load management, the system operator is allowed to use the DLC program for some loads. Three types of residential, commercial and industrial loads are considered in the model and the priority of load supply is for industrial, residential and commercial loads, respectively. Three types of residential, commercial and industrial loads are considered into account and the priority is to supply industrial loads. It is noteworthy that the contingent event is a storm and the scenarios are generated based on the weather forecast and equipment vulnerability analysis. During the event, the system operator will be able to reduce the load interruption by changing the status of the network switches, utilizing the DLC program, and switching to island mode. Finally, the model is implemented on a 69-bus distribution system and the effect of the proposed model on load supply and operating cost is studied in detail. The contributions are:

- Providing a MILP framework for resilience enhancement of distribution system using automatic switching;
- Considering three types of residential, commercial and industrial loads with different priority in the network;
- Investigating the effect of switching on supplying higher priority loads under critical conditions;
- Investigating the effect of DLC program on load recovery under critical conditions;
- Evaluating the effect of EES systems on load recovery under critical conditions.

The rest of this paper is as follows: Section II presents the modified IEEE 69-bus distribution system. Section III represents the mathematical formulation of the model. In section IV, the proposed model is solved in the form of 4 case studies and its results are discussed. Finally, some concluded remarks are presented in section V.

II. The Overview of Studied System

The overview of the studied system is presented in Fig. 1. As can be seen, four gas turbines and five wind turbines are located on the grid. An EES system is installed next to each wind turbine to not only increase the flexibility of the system but also to prevent power curtailment of the wind turbines.

There is a sectionalizing at both ends of each line and also four tie-lines are installed in the network. It should be noted that the system operator will be able to change the network topology by changing the status of the switches and thus change the power supply path. In the studied network, three types of loads are considered, which include industrial, residential and commercial loads. It should be mentioned that under critical conditions, industrial loads are considered as vital loads and after that, the priority of supply is with residential and commercial loads, respectively.

III. Mathematical Modelling

In this section, mathematical modeling of the proposed model is presented.

$$\max OF = \sum_{s} \rho_s \left[\begin{array}{l} \sum_{n\in N^{Ind}} \omega^{Ind} \left(\sum_{t} \left(\alpha_{s,n,t} - \gamma_{s,n,t} \right) P_{s,n,t}^{Load} \Delta t \right) \\ + \sum_{n\in N^{Com}} \omega^{Com} \left(\sum_{t} \gamma \left(\alpha_{s,n,t} - \gamma_{s,n,t} \right) P_{s,n,t}^{Load} \Delta t \right) \\ + \sum_{n\in N^{Res}} \omega^{Res} \left(\sum_{t} \left(\alpha_{s,n,t} - \gamma_{s,n,t} \right) P_{s,n,t}^{Load} \Delta t \right) \end{array} \right] \quad (1)$$

$$\sum_{g\in G^n} P_{s,g,t}^{Gen} + \sum_{w\in W^n} P_{s,w,t}^{Wind} + \sum_{m} P_{s,m\to n,t}^{Line} + \sum_{e\in E^n} P_{s,e,t}^{Dch} = \sum_{m} P_{s,n\to m,t}^{Line} + \left(\alpha_{s,n,t} - \gamma_{s,n,t} \right) P_{s,n,t}^{Load} + \sum_{e\in E^n} P_{s,e,t}^{Ch} \quad (2)$$

$$\sum_{g\in G^n} Q_{s,g,t}^{Gen} + \sum_{m} Q_{s,m\to n,t}^{Line} = \sum_{m} Q_{s,n\to m,t}^{Line} + \left(\alpha_{s,n,t} - \gamma_{s,n,t} \right) Q_{s,n,t}^{Load} \quad (3)$$

$$-P_{n\to m}^{Line,Max} \upsilon_{s,m\to n,t} \le P_{s,n\to m,t}^{Line} \le P_{n\to m}^{Line,Max} \upsilon_{s,n\to m,t} \quad (4)$$

$$-Q_{n\to m}^{Line,Max} \upsilon_{s,m\to n,t} \le Q_{s,n\to m,t}^{Line} \le Q_{n\to m}^{Line,Max} \upsilon_{s,n\to m,t} \quad (5)$$

$$V_{s,m,t} \ge V_{s,n,t} - \frac{R_{n\to m} P_{s,n\to m,t} + X_{n\to m} Q_{s,n\to m,t}}{V_0} - \left(1 - I_{s,n\to m,t}^{Line} \right) M \quad (6)$$

$$V_{s,m,t} \le V_{s,n,t} - \frac{R_{n\to m} P_{s,n\to m,t} + X_{n\to m} Q_{s,n\to m,t}}{V_0} + \left(1 - I_{s,n\to m,t}^{Line} \right) M \quad (7)$$

$$\upsilon_{s,m\to n,t}, \upsilon_{s,n\to m,t}, I_{s,n\to m,t}^{Line} \in \{0,1\} \quad (8)$$

$$V_n^{Min} \le V_{s,n,t} \le V_n^{Max} \quad (9)$$

$$0 \le \gamma_{s,n,t} \le \gamma_n^{Max} \alpha_{s,n,t} \qquad n \in N^{DLC} \quad (10)$$

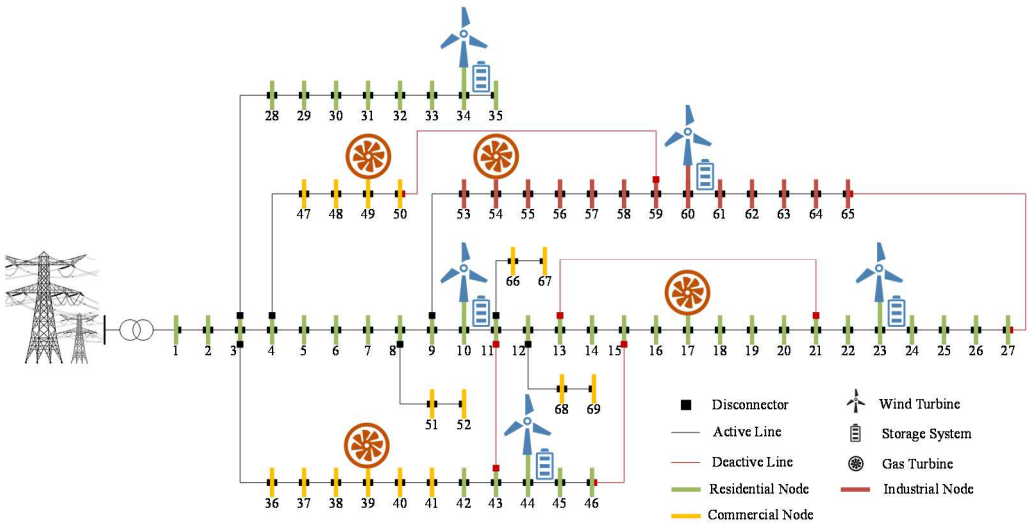

Fig. 1. The overview of modified IEEE 69-bus distribution system.

$$\upsilon_{s,m\to n,t}+\upsilon_{s,n\to m,t}=I^{Line}_{s,n\to m,t} \tag{11}$$

$$1-\kappa_{n\to m}\le I^{Line}_{s,n\to m,t}\le 1 \tag{12}$$

$$\sum_{n\to m}\left(1-I^{Line}_{s,n\to m,t}\right)\ge \beta^{Off,Min} \tag{13}$$

$$\sum_{m}\upsilon_{s,m\to n,t}\le 1 \tag{14}$$

$$\sum_{t}\sum_{n\to m}\left|I^{Line}_{s,n\to m,t}-I^{Line}_{s,n\to m,t-1}\right|\le N^{SW} \tag{15}$$

$$\sum_{t}\left|I^{Line}_{s,n\to m,t}-I^{Line}_{s,n\to m,t-1}\right|\le N^{SW}_{n\to m} \tag{16}$$

$$I^{Line,On}_{s,n\to m,t}-I^{Line,Off}_{s,n\to m,t}=I^{Line}_{s,n\to m,t}-I^{Line}_{s,n\to m,t-1} \tag{17}$$

$$0\le I^{Line,On}_{s,n\to m,t}+I^{Line,Off}_{s,n\to m,t}\le 1 \tag{18}$$

$$\left|I^{Line}_{s,n\to m,t}-I^{Line}_{s,n\to m,t-1}\right|=I^{Line,On}_{s,n\to m,t}+I^{Line,Off}_{s,n\to m,t} \tag{19}$$

$$I^{Line}_{s,n\to m,t}=\alpha_{s,n,t}\ \alpha_{s,m,t}\ J^{Line}_{s,n\to m,t}+\bar{J}^{Line}_{s,n\to m,t}\ge I^{Line}_{s,n\to m,t} \tag{20}$$

$$J^{Line}_{s,n\to m,t}=\alpha_{s,n,t}\alpha_{s,m,t}\Rightarrow\begin{cases}J^{Line}_{s,n\to m,t}\le\alpha_{s,n,t}\\ J^{Line}_{s,n\to m,t}\le\alpha_{s,m,t}\\ J^{Line}_{s,n\to m,t}\ge\alpha_{s,n,t}+\alpha_{s,m,t}-1\end{cases} \tag{21}$$

$$\bar{J}^{Line}_{s,n\to m,t}=\left(1-\alpha_{s,n,t}\right)\left(1-\alpha_{s,m,t}\right)\Rightarrow\begin{cases}\bar{J}^{Line}_{s,n\to m,t}\le 1-\alpha_{s,n,t}\\ \bar{J}^{Line}_{s,n\to m,t}\le 1-\alpha_{s,m,t}\\ \bar{J}^{Line}_{s,n\to m,t}\ge 1-\alpha_{s,n,t}-\alpha_{s,m,t}\end{cases} \tag{22}$$

$$\kappa_{n\to m},\alpha_{s,n,t},J^{Line}_{s,n\to m,t},\bar{J}^{Line}_{s,n\to m,t}\in\{0,1\} \tag{23}$$

$$P^{Gen,Min}_{g}I^{Gen}_{s,g,t}\le P^{Gen}_{s,g,t}\le P^{Gen,Max}_{g}I^{Gen}_{s,g,t} \tag{24}$$

$$Q^{Gen,Min}_{g}I^{Gen}_{s,g,t}\le Q^{Gen}_{s,g,t}\le Q^{Gen,Max}_{g}I^{Gen}_{s,g,t} \tag{25}$$

$$P^{Wind,Max}_{s,w,t}=\begin{cases}0 & ,0\le v_{s,w,t}\le v^{Cut-In}_{w}\\ (a+v_{s,w,t}b+v^{2}_{s,w,t}c)P^{Wind,Rated}_{s,w} & ,v^{Cut-In}_{w}\le v_{s,w,t}\le v^{Rated}_{w}\\ P^{Wind,Rated}_{s,w} & ,v^{Rated}_{w}\le v_{s,w,t}\le v^{Cut-Off}_{w}\\ 0 & ,v_{s,w,t}\ge v^{Cut-Off}_{w}\end{cases} \tag{26}$$

$$0\le P^{Wind}_{s,w,t}\le P^{Wind,Max}_{s,w,t} \tag{27}$$

$$E_{s,e,t}=E_{s,e,t-1}+\left(P^{Ch}_{s,e,t}\eta^{Ch}_{e}-\frac{P^{Dch}_{s,e,t}}{\eta^{Dch}_{e}}\right)\Delta t \tag{28}$$

$$E_{s,e,t=1}=E_{s,e,t=24}=SOC^{Initial}_{e}E^{Max}_{e} \tag{29}$$

$$SOC^{Min}_{e}\le\frac{E_{s,e,t}}{E^{Max}_{e}}\le SOC^{Max}_{e} \tag{30}$$

$$0\le P^{Ch}_{s,e,t}\le P^{Ch,Max}_{e}\left(SOC^{Max}_{e}E^{Max}_{e}-E_{s,e,t}\right) \tag{31}$$

$$0\le P^{Dch}_{s,e,t}\le P^{Dch,Max}_{e}\left(E_{s,e,t}-SOC^{Min}_{e}E^{Max}_{e}\right) \tag{32}$$

$$0\le P^{Ch}_{s,e,t}\le P^{Ch,Max}_{e}I^{Ch}_{s,e,t} \tag{33}$$

$$0\le P^{Dch}_{s,e,t}\le P^{Dch,Max}_{e}I^{Dch}_{s,e,t} \tag{34}$$

$$0\le I^{Ch}_{s,e,t}+I^{Dch}_{s,e,t}\le 1 \tag{35}$$

Eq. (1) presents the objective function, which is modeled as load supply maximization. In the proposed model, network loads are divided into three types: industrial, commercial and industrial, which in the objective function, according to their priority, a weight coefficient is considered for each of them. It is assumed that industrial loads have the highest priority in this research. $\alpha_{s,n,t}$ is a binary variable that indicates the connection of each node. ρ_s and $\gamma_{s,n,t}$ are the probability of occurrence of each scenario and the percentage of load shortage at each node, respectively. The power flow constraints are presented in Eqs. (2)-(13) [8]. In this regard, Eqs. (2) and (3) represent the active and reactive power constraints, respectively.

Eq. (2) states that the sum of the power generated, input and discharged by the EES in each node must be equal to the sum of the power consumed, charged and curtailed by the DLC program at the same node. Constraints (4) and (5) restricted the active and reactive power passing through each line, respectively. $\upsilon_{s,n\to m,t}$ and $\upsilon_{s,m\to n,t}$ are binary variables that determine the direction of power passing through each line. Eqs. (6) and (7) express the relationship between the power passing through each line and the voltage at its two ends. $I^{Line}_{s,n\to m,t}$ is a binary variable that indicates the active/deactive status of each line. It is assumed that n is the power sender bus and m is the power receiver bus. In order to linearize these equations, the BigM method has been used. It should be noted that for inactive lines, these equations will be relaxed. Eq. (8) shows the binary variables, and constraint (9) models the voltage magnitude limits at each bus. Constraint (10) states that the load interruption rate by the DLC program in each node cannot be more than a predetermined value [9]. It is assumed that the distribution system operator is only allowed to use the DLC program in nodes with a load greater than 100 kW.

Constraint (11) states that for each active line, the binary variable corresponding to its status is activated. Besides, constraint (12) guarantees the activation of lines that do not have switches. $\kappa_{n\to m}$ is the input parameter that determines the presence of the switch in each line. In order to increase the computational speed, constraint (13) determines the minimum number of inactive lines according to the total number of lines. It should be noted that due to the possibility of forming an island in the network, the maximum number of inactive lines is not limited. Constraint (14) guarantees the radiality of the network after switching [10]. Finally, constraints (15) and (16) limit the number of switches per line and during operation.

Due to the use of the absolute value function in constraints (15) and (16), the model is nonlinear. Therefore, in Eqs. (17)-(19), the equations required to linearize these constraints are presented. In this regard, in Eq. (17), the status of activation/deactivation of each line is determined by the binary variables ($I^{Line,On}_{s,n\to m,t}$ and $I^{Line,Off}_{s,n\to m,t}$). Eq. (18) states that if the line status does not change, its binary variables must be equal to zero. Finally, the absolute value of these binary variables is calculated through Eq. (19).

Eq. (20) states that if a line is active, the binary variables of the nodes connected to its two ends ($\alpha_{s,n,t}$ and $\alpha_{s,m,t}$) must be active simultaneously, and vice versa. $J^{Line}_{s,n\to m,t}$ and $\bar{J}^{Line}_{s,n\to m,t}$ are auxiliary variables used to linearize the XNOR function. It is noteworthy that if the binary variables at both ends of each line are active at the same time, the value of $J^{Line}_{s,n\to m,t}$ is equal to 1, while if the mentioned binary variables are simultaneously inactive, the value of will be equal to 1. In Eqs. (21)-(23), the constraints required to linearize Eq. (20) are presented. Constraints (24) and (25) model the active and reactive power generated by gas turbines, respectively. The power output by the wind turbine is also calculated by the four-part function presented in Eq. (26), which depends on the hourly wind speed and the characteristics of the turbine. Constraint (27) also limits the maximum wind turbine generation capacity.

EES operating constraints are presented in (28)-(36) [11], [12]. The energy level of the EES per hour is calculated by Eq. (28), which is a function of the energy stored from the previous hour and the charged/discharged power in the current hour. Constraints (29) states that the energy level of EES at the start and end hours of operation must be equal. Constraint (30) limits the minimum and maximum state of charge (SoC) of the EES. Constraint (31) states that increasing the SoC of the EES system leads to a lower charge speed and vice versa. Constraint (32) also applies this restriction to the discharge operating mode. Constraints (33) and (34) model the charge and discharge limits, respectively. Finally, constraint (35) is provided to prevent simultaneous charging and discharging of EES.

IV. Simulation Results

In this section, the proposed model is implemented on a modified IEEE 69-bus distribution system and is solved in the form of 4 case studies according to Table I. In order to analyze the performance of the proposed model under critical situations, three events include; disconnecting from the upstream grid, wind turbines outage and the outage of line 7 (between buses 7 and 8) are considered, and case studies are resolved under these conditions. In this study, it is assumed that the duration of events is 8 hours (between 13-20 hours). Tables II and III present the data required for the simulation and location of equipment, respectively. It should be noted that load demand and wind speed uncertainties have been considered and the problem has been modelled as a scenario-based optimization problem. In this regard, first, 1000 scenarios were generated for load demand and wind speed by the beta and Weibull distribution functions, respectively, and then to reduce the computational burden, the number of initial scenarios was reduced to 10 by the backward scenario reduction algorithm. The reduced scenarios are presented in Fig. 2.

TABLE I. The List of Case Studies

Case No.	Network Topology		DLC Program	EES
	Fixed	Dynamic		
1	✓	×	×	×
2	×	✓	×	×
3	×	✓	✓	×
4	×	✓	✓	✓

TABLE II. The Required Data for Simulation

Parameter	Value	Parameter	Value
Total Active Power	3802.1 kW	N^{SW}	20
Total Reactive Power	2694.7 kVar	$N^{SW}_{n\to m}$	6
V_n^{Min}	0.9 p.u.	ω^{Ind}	0.5
V_n^{Max}	1.1 p.u.	ω^{Res}	0.3
η_e^{Ch} / η_e^{Dch}	95%	ω^{Com}	0.2
SOC_e^{Min}	30%	V_0	12.7 kV
SOC_e^{Max}	90%	v_w^{Cut-In}	5 m/s
$P_e^{Ch,Max}$	40%	v_w^{Rated}	14 m/s
$P_e^{Dch,Max}$	45%	$v_w^{Cut-Off}$	20 m/s
$SOC_e^{Initial}$	50%	γ_n^{Max}	0.7

TABLE III. Location and Capacity of DERs and EES Systems

Location	Type	Capacity (kW)	Location	Type	Capacity (kW)
Bus 10	WT	400	Bus 39	GT	500
Bus 10	EES	160	Bus 44	WT	500
Bus 17	GT	400	Bus 44	EES	200
Bus 23	WT	400	Bus 49	GT	300
Bus 23	EES	160	Bus 54	GT	300
Bus 34	WT	400	Bus 60	WT	500
Bus 34	EES	160	Bus 60	EES	200

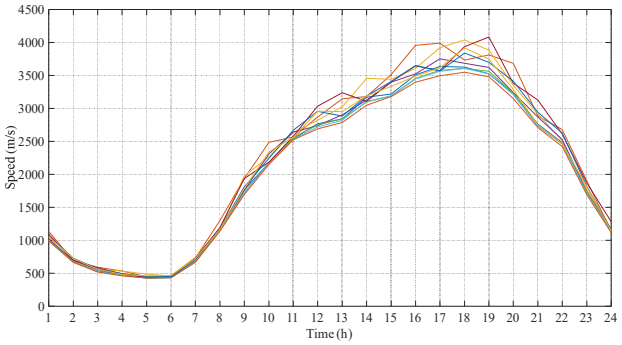

(a) Load demand

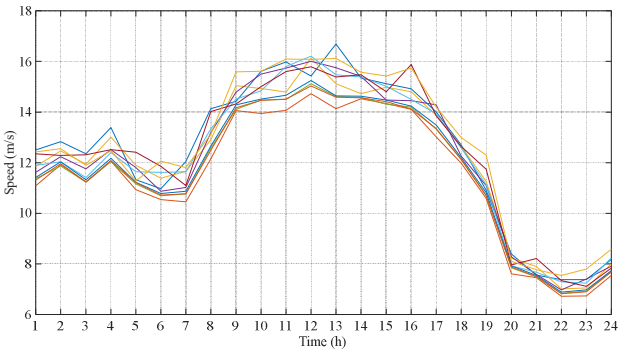

(b) Wind speed

Fig. 2.The obtained scenarios for demand and wind speed.

Tables IV-VI present the operation results during the abovementioned critical conditions. Table IV presents the results of case studies 1-4 during disconnecting from the upstream grid.

As can be seen, the amount of ENS, as well as the amount of loads curtailed by the DLC program, is provided per hour. It should be noted that the penalty cost paid for ENS is much higher than the cost of using the DLC program. In addition, the system operator can supply higher priority loads by applying the DLC program to lower priority loads. Comparison of cases 1 and 2 indicates that in case 2 the amount of ENS has decreased significantly, which is due to automatic switching after the occurrence of the events. Numerical results demonstrate that the total amount of ENS in case 2 has decreased by 12.45% compared to case 1.

Analysis of the results of case 3 also demonstrates that the use of the DLC program has led to a significant reduction in ENS. It should be noted that the DLC program is modeled as a bi-lateral contract between the customers and the distribution system operator, which by applying it, the system operator will be able to curtail part of the customer's load in exchange for a predetermined fee.

TABLE IV. THE OBTAINED RESULTS DURING DISCONNECTING FROM UPSTREAM-GRID: CASES 1-4

Hour	ENS (kWh)				DLC (kWh)	
	Case1	Case2	Case3	Case4	Case3	Case4
13	591.15	255.95	105.88	0	113.4	0
14	897.7	528.24	116.7	0	141.59	109.39
15	1003.95	750.71	119.99	0	231.72	220.54
16	1556.2	1308.4	129.44	87.34	462.2	424.32
17	1921.14	1391.68	133.82	90.3	626.91	555.58
18	1946.7	2224.4	135.6	91.5	800.08	757.89
19	1903.44	2174.97	132.59	89.47	872.7	794.16
20	1730.4	1477.33	120.53	202.31	871.03	705.51
Sum	11550.67	10111.67	994.54	560.92	4119.61	3567.4

Finally, the results obtained for case 4 show that the presence of EES systems has led to a 43.6% and 13.4% reduction in ENS and DLC amounts, respectively. The results of case 4 substantiated that EES systems enhance system resilience.

Table V presents the operating results during the outage of wind turbines. Comparison of the results with Table IV shows that the connection of the distribution system to the upstream grid has led to a greater effect of switching on reducing the amount of ENS. Numerical results illustrate that automatic switching during disconnecting from the upstream grid leads to a 12.45% reduction in ENS, while automatic switching during wind turbines outage has reduced the ENS by about 16.17%. Therefore, the results show that upstream network connection and automatic switching have a high impact on reducing ENS in critical conditions. Table VI presents the operating results during the outage of Line 7. The results of the table indicate that the effect of automatic switching on the decrease in the amount of ENS during the outage of this line was much greater than previous events. Numerical results illustrate a decrease of 93.25% of the ENS. It should be noted that in case 1, due to the impossibility of automatic switching, the network was not able to supply the loads located on this line.

TABLE V. THE OBTAINED RESULTS DURING DISCONNECTING FROM UPSTREAM-GRID: CASES 1-4

Hour	ENS (kWh)				DLC (kWh)	
	Case1	Case2	Case3	Case4	Case3	Case4
13	0	0	0	0	0	0
14	48.19	0	0	0	0	0
15	155.11	0	0	0	64.28	41.72
16	408.93	258.87	87.34	0	241.94	268.58
17	483.66	544.36	90.3	0	361.87	279.09
18	560	629.4	91.5	91.5	410.6	282.8
19	448.51	462.1	89.47	89.47	328.14	251.61
20	155.82	0	0	0	79.64	38.73
Sum	2260.23	1894.73	358.61	180.97	1486.48	1162.52

TABLE VI. THE OBTAINED RESULTS DURING DISCONNECTING FROM UPSTREAM-GRID: CASES 1-4

Hour	ENS (kWh)				DLC (kWh)	
	Case1	Case2	Case3	Case4	Case3	Case4
13	1452.62	71.83	0	0	71.83	0
14	1601.07	76.34	0	0	76.34	0
15	1646.17	80.44	0	0	80.44	0
16	1716.56	9.8	0	0	9.8	0
17	1802.32	139.49	90.3	0	49.2	0
18	1963.4	353.84	91.5	0	262.34	27.61
19	1760.39	177.9	89.47	0	88.43	0
20	1545.16	0	0	0	0	0
Sum	13487.68	909.64	271.27	0	638.38	27.61

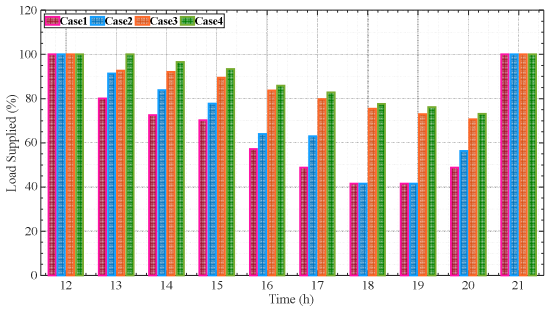

Fig. 3. The amount of load supplied during disconnecting from the upstream grid: Cases 1-4.

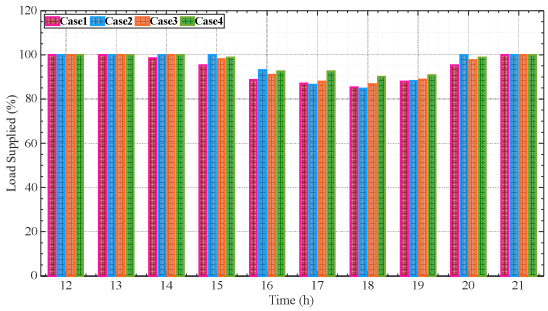

Fig. 4. The amount of load supplied during the outage of wind turbines: Cases 1-4.

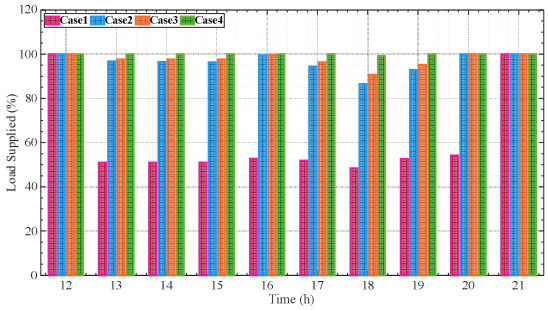

Fig. 5. The amount of load supplied during the outage of line 7: Cases 1-4.

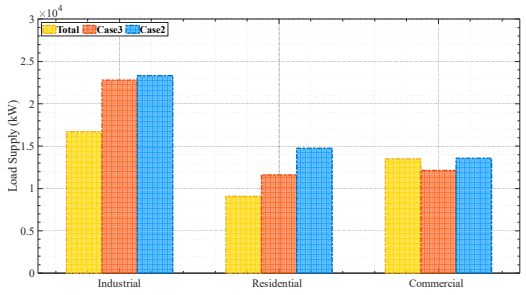

Fig. 6. The amount of industrial, residential and commercial loads supplied during disconnecting from the upstream-grid: Cases 2-3.

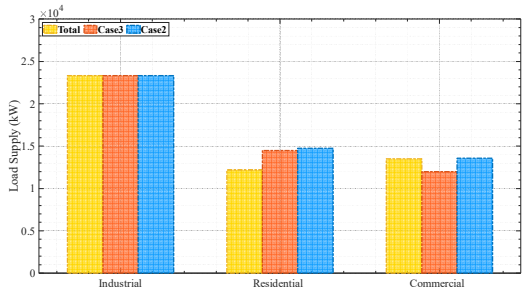

Fig. 7. The amount of industrial, residential and commercial loads supplied during the outage of wind turbines: Cases 2-3.

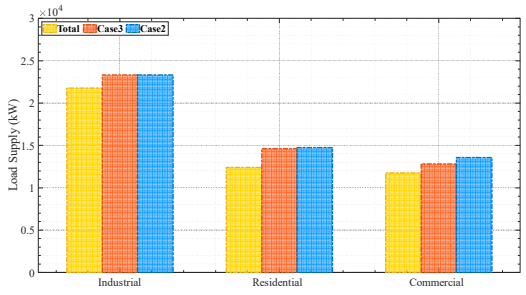

Fig. 8. The amount of industrial, residential and commercial loads supplied during the outage of line 7: Cases 2-3.

Figs. 3-5 depict the amount of load supplied during different events. As these figures show, during all events, the highest load supplied was in Case 4, which is due to the possibility of automatic switching, the use of DLC program and the presence of EES systems. In order to investigate the effect of DLC program on curtail of lower priority loads and supply of higher priority loads, in Figs. 6-8, the amount of industrial, residential and commercial loads supplied in cases 2 and 3 are compared. As can be seen from the figures, the application of the DLC program has led to the curtailment of some commercial and residential loads and in return the supply of more industrial loads. Therefore, the results of this section prove the high impact of the DLC program on the supply of vital loads (industrial loads).

V. Conclusion

In this paper, a scenario-based model was proposed to maximize network load supply under critical conditions, through automatic switching and utilization of the DLC program. The studied system was a modified IEEE 69-bus distribution system, on which industrial, residential and commercial loads with different supply priorities were considered. The proposed model was solved in the form of four case studies and the effect of automatic switching, DLC program and EES systems on the load supply was investigated in detail. Initially, the simulation results demonstrated that automatic switching by changing the network topology leads to a significant increase in the load supplied during critical conditions. Numerical results illustrated that automatic switching has led to a reduction of 12.45%, 16.17% and 93.25% of the ENS during disconnection from the upstream-grid, wind turbines outage and the outage of line 7, respectively. In addition, the results demonstrated that the use of DLC program has led to the curtailment of some lower priority loads (residential and commercial loads) and, conversely, increased supply of higher priority loads (industrial loads). Finally, the results indicated that the presence of EES systems significantly reduces the amount of ENS and thus enhances system resilience. Overall, the results showed that the proposed model significantly reduces the amount of ENS and also supplied a greater amount of vital loads in critical conditions.

References

[1] S. Pandey, S. Chanda, A. K. Srivastava, and R. O. Hovsapian, "Resiliency-Driven Proactive Distribution System Reconfiguration With Synchrophasor Data," *IEEE Trans. Power Syst.*, vol. 35, no. 4, pp. 2748–2758, 2020, doi: 10.1109/TPWRS.2020.2968611.

[2] Q. Shi *et al.*, "Network reconfiguration and distributed energy resource scheduling for improved distribution system resilience," *Int. J. Electr. Power Energy Syst.*, vol. 124, p. 106355, 2021, doi: https://doi.org/10.1016/j.ijepes.2020.106355.

[3] Y. Wang, Y. Xu, J. Li, J. He, and X. Wang, "On the Radiality Constraints for Distribution System Restoration and Reconfiguration Problems," *IEEE Trans. Power Syst.*, vol. 35, no. 4, pp. 3294–3296, 2020, doi: 10.1109/TPWRS.2020.2991356.

[4] M. J. Reno, "Impact study of demand response program on the resilience of dynamic clustered distribution systems," *IET Gener. Transm. Distrib.*, vol. 14, no. 22, pp. 5230-5238(8), Nov. 2020.

[5] I. Husain, "Utilising demand response for distribution service restoration to achieve grid resiliency against natural disasters," *IET Gener. Transm. Distrib.*, vol. 13, no. 14, pp. 2942-2950(8), Jul. 2019.

[6] C. Qin, "Unified two-stage reconfiguration method for resilience enhancement of distribution systems," *IET Gener. Transm. Distrib.*, vol. 13, no. 9, pp. 1734-1745(11), May 2019.

[7] S. Lei, C. Chen, H. Zhou, and Y. Hou, "Routing and Scheduling of Mobile Power Sources for Distribution System Resilience Enhancement," *IEEE Trans. Smart Grid*, vol. 10, no. 5, pp. 5650–5662, 2019, doi: 10.1109/TSG.2018.2889347.

[8] S. A. Mansouri, A. Ahmarinejad, E. Nematbakhsh, M. S. Javadi, A. R. Jordehi, and J. P. S. Catalão, "Energy Management in Microgrids including Smart Homes: A Multi-objective Approach," *Sustain. Cities Soc.*, p. 102852, 2021, doi: https://doi.org/10.1016/j.scs.2021.102852.

[9] S. A. Mansouri, A. Ahmarinejad, M. S. Javadi, A. E. Nezhad, M. Shafie-Khah, and J. P. S. Catalão, "Chapter 9 - Demand response role for enhancing the flexibility of local energy systems," G. Graditi and M. B. T.-D. E. R. in L. I. E. S. Di Somma, Eds. Elsevier, 2021, pp. 279–313.

[10] A. Azizivahed, H. Lotfi, M. J. Ghadi, S. Ghavidel, L. Li, and J. Zhang, "Dynamic Feeder Reconfiguration in Automated Distribution Network Integrated with Renewable Energy Sources with Respect to the Economic Aspect," in *2019 IEEE PES Innovative Smart Grid Technologies Asia, ISGT 2019*, 2019, pp. 2666–2671, doi: 10.1109/ISGT-Asia.2019.8881503.

[11] S. A. Mansouri, A. Ahmarinejad, M. S. Javadi, and J. P. S. Catalão, "Two-stage stochastic framework for energy hubs planning considering demand response programs," *Energy*, vol. 206, p. 118124, 2020, doi: 10.1016/j.energy.2020.118124.

[12] S. A. Mansouri, A. Ahmarinejad, M. Ansarian, M. S. Javadi, and J. P. S. Catalao, "Stochastic planning and operation of energy hubs considering demand response programs using Benders decomposition approach," *Int. J. Electr. Power Energy Syst.*, vol. 120, p. 106030, 2020, doi: 10.1016/j.ijepes.2020.106030.